Laminar and Turbulent Flow of Unstable Liquid-Liquid Emulsions

J. A. CENGEL, A. A. FARUQUI, J. W. FINNIGAN, C. H. WRIGHT, and J. G. KUNDSEN

Oregon State University, Corvallis, Oregon

Liquid-liquid dispersions containing various volume fractions of a petroleum solvent dispersed in water have been studied in laminar and turbulent flow conditions. If one assumes that the dispersion behaves as a single-phase fluid, measured friction factors may be used to calculate an effective viscosity of the mixture.

In laminar flow, viscosities were found to be a function of capillary diameter, possibly due to the formation of a thin film of continuous phase adjacent to the capillary wall. The thickness of this film was determined to be of the order of 10 to 25 μ, which is probably of the order of the average size of the droplets.

Up to 20% solvent, the relative fluidity (or viscosity) of the dispersions was the same in laminar, vertical turbulent, and horizontal turbulent flow. In the laminar flow case viscosity decreased somewhat with flow rate and became essentially constant at a Reynolds number of about 1,000.

In vertical turbulent flow all dispersions behaved as Newtonian fluids, and a single curve (Figure 6) is presented to predict fluidities. The 35 and 50% dispersions in horizontal flow exhibited non-Newtonian characteristics and had effective fluidities considerably less than the same dispersion in vertical flow but agreed with the horizontal turbulent flow results of Baron, et al. The apparent non-Newtonian behavior could be due to phase separation in the horizontal tube.

Corrected laminar flow fluidities for dispersions with 35 and 50% solvent deviated from the vertical turbulent flow results. Reasons for this are unexplained. In laminar flow also, tube orientation affected the viscosity of the 50% dispersion.

This paper describes an investigation of the apparent viscosity of an unstable liquid-liquid dispersion under conditions of laminar and turbulent flow in a circular tube. The dispersion was made up of a kerosenelike petroleum solvent dispersed in water.

The rheological properties of two-phase fluids are of prime importance in processes where two phases contact each other. Gas-solid, gas-liquid, and liquid-solid systems have been studied extensively since these systems are frequently encountered in absorption, fluidization, and vaporization operations. In operations in which one liquid contacts another a liquid-liquid dispersion or emulsion often must be handled. Research described in this paper was undertaken to obtain information on the apparent viscosity of liquid-liquid dispersions under various conditions of flow.

PREVIOUS WORK

For the laminar flow of Newtonian fluids the shear stress is proportional to the rate of shear:

$$\tau = \frac{\mu}{g_c}\frac{du}{dy} \qquad (1)$$

The constant of proportionality μ is called the viscosity of the fluid. Some dispersions (*1*) and suspensions (*16*) can be treated as Newtonian fluids, while other suspensions (*13, 14*) are non-Newtonian and do not exhibit this proportionality between shear stress and rate of shear. The viscosity of Newtonian dispersions and suspensions depends upon several factors (*2*):

1. Volume concentration of dispersed phase.
2. Viscosities of continuous and dispersed phases.
3. Size and shape of dispersed particles.
4. Distribution of particles.
5. Interfacial tension.
6. Temperature.

In general, as the concentration of the dispersed phase increases, viscosity increases to a maximum value where inversion occurs (in the case of two liquids) because of the interchange of phases; that is the former dispersed phase becomes the continuous phase. Suspensions of solid particles ultimately attain infinite viscosity as the concentration approaches that of the settled volume of the mass of particles.

Considerable theoretical and empirical work has been done in correlating the viscosity of suspensions with some of the variables mentioned above. For suspensions of uniform, randomly distributed spheres in a liquid at low concentrations Einstein (*4, 5*) derived the following relationship between the viscosity of the suspension μ_m and the volume fraction:

$$\mu_m = \mu_c\,(1 + 2.5\,\phi) \qquad (2)$$

Many subsequent investigators expanded Equation (2) into polynomial form

$$\mu_m = \mu_c\,(1 + k\phi + a\phi^2 + b\phi^3 + \ldots) \qquad (3)$$

and determined constants that would fit their data. In some cases the value of k used in Equation (3) has been 2.5, but in others it has ranged from 1.5 to 18. Values of a and b in Equation (3) are reported in the range of 4.6 to 14.1 and 8.8 to 40, respectively. An example of a polynomial relation is that of Vand (*21*):

$$\mu_m = \mu_c\,[1 + 2.5\phi + 7.349\phi^2 + 16.2\phi^3] \qquad (4)$$

Logarithmic and exponential relationships have also been proposed but usually are applicable only to specific dispersions. The empirical relationship of Roscoe (*18*)

$$\mu_m = \mu_c(1 - \phi)^{-2.5} \qquad (5)$$

describes the viscosity of a suspension of many sized particles.

The above relationships apply to suspensions of solid particles. When the dispersed phase is a fluid, its viscosity and the interfacial tension between the phases must be considered. The effect of these two variables has been considered theoretically by Taylor (*19*) and Oldroyd (*15*). Results of these workers however are applicable only for low concentrations. Recently Ford (*8*) compared the various theoretical and experimental results on viscosities of suspensions and proposed relationships in terms of relative fluidities (μ_c/μ_m) rather than relative viscosity. This has merit, particularly for suspensions of solids, because as the dispersed phase concentration increases to the so-called *settled volume* of the particles, the viscosity becomes infinite so that the fluidity becomes zero. The fluidity-concentration curve therefore has a definite intercept on the concentration axis. As the concentration approaches zero, Equation (2) becomes

$$\mu_c/\mu_m = 1 - 2.5\,\phi \qquad (6)$$

Curve *A* in Figure 1 represents many of the experimental results for the fluidities of suspensions of randomly distributed uniform spheres. Much of the data scatters widely at high concentrations. Zero fluidity is attained at $\phi = 0.55$, which is very close to 0.524, which corresponds to cubic packing of uniform spheres. The curve *A* also approaches zero concentration at a slope of -2.5. In fact it agrees with Equation (6) at concentrations up to 15% solids.

If the relative fluidity of a suspension of solid or liquid particles deviates

J. A. Cengel is at Purdue University, Lafayette, Indiana. J. W. Finnigan is with the General Electric Company, Richland, Washington. C. H. Wright is with the Thiokol Chemical Corp., Brigham City, Utah.

considerably from curve A, such deviation could be caused by nonspherically shaped particles, nonuniform size distribution, finite viscosity of the dispersed phase, and interfacial tension. For example curve B in Figure 1 gives the relative fluidity of nonuniform spheres as reported by Happel (9), and curve C is the relative fluidity of an aluminum powder suspension investigated by Orr and Dallavalle (16). If the suspension contains deformable particles (such as latex), one might expect the point of zero fluidity to occur at considerably higher concentrations than 0.55. This has been shown in investigations of asphalts and latex suspensions.

EXPERIMENTAL APPARATUS

A schematic flow sheet of the experimental apparatus is shown in Figure 2. The dispersion was prepared in a stainless steel, jacketed mixing tank where temperature could be maintained constant by cooling water. Except for the test section, the system was made of 1¼-in. standard brass pipe. Circulation was provided by a turbine pump equipped with a bypass to the mixing tank to control flow and bring about additional mixing of the dispersion. A flow orifice was included in the system to measure the flow rate.

Horizontal turbulent flow friction factor data were obtained in a 10½ ft. long test section of ⅞ in. O.D., 16 Birmingham wire gauge copper tubing. For determining friction losses, pressure taps were located 4 and 10 ft. from the entrance to the copper tube. Vertical turbulent flow friction factor data were obtained in a 9½ ft. long test section of the same tabing as the horizontal section. Pressure taps were 6 ft. apart, the calming length before the upstream tap being 35 in. Pressure differentials were measured by either mercury or carbon tetrachloride under water. Each manometer line was equipped so that it could be flushed with water to remove any emulsion or air that might have entered the pressure transmission lines.

Figure 2 shows the arrangement for measuring viscosity during laminar flow. Since the dispersion was unstable, it was not possible to study it under static conditions. The system consists of a capillary tube and a pressure gauge installed in a straight portion of the circulation system. Glass capillary tubes were inserted at right angles to the flowing system so that the end of the tube was located at the pipe axis. The pressure tap diametrically across from the capillary tube was connected to a stainless steel Bourdon pressure gauge with an 8-in. face marked in 0.05 lb./sq. in. divisions. The capillary tube was held in place by a brass fitting equipped with a packing gland and nut. The several capillary tubes used for viscosity measurements are described in Figure 3. Diameters of the capillary tubes were measured by weighing the amount of mercury required to fill the tubes. Viscosity of pure water determined with the tubes agreed well with published data, indicating the diameter had been measured accurately by this method. Two orientations of the capillary viscometer were employed:

1. Downward flow in main pipe and horizontal flow in capillary.
2. Horizontal flow in main pipe and downward flow in capillary.

Fluid discharged from the capillary into a weighing cup and the time of discharge was obtained by means of a stopwatch.

At all times water was the continuous phase. The properties of the solvent at 71°F. are as follows: ρ = 48.8 lb.$_m$/cu. ft., C_p = 0.468 B.t.u./lb.$_m$ °F., k = 0.109 B.t.u./(hr.)(sq. ft.) °F./ft., μ = 0.976 centipoises, IBP = 304°F., FBP = 362°F. Compositions investigated ranged from 5 to 50% (by volume) solvent, in addition to water and pure solvent. Complete experimental data are available (3, 7, 22).

To prepare the dispersions a known weight of solvent was added to a previously weighed amount of water in the mixing tank. The time necessary to achieve a thorough blending of the two liquids was usually 2 to 3 hr. The dispersion had a milk-white appearance, characteristic of many liquid-liquid emulsions. The phases separated readily and completely when agitation ceased.

During the tests agitation of the emulsion was accomplished by the propeller stirrer in the mixing tank and by bypassing a certain amount of the pump discharge. The level of agitation was maintained sufficiently high so that the mixture in the tank appeared uniform and no layer of solvent was apparent on the surface of the mixture.

ANALYSIS AND DISCUSSION

As the dispersion was circulated in the system, it was in a state of dynamic equilibrium with coalescence and breakup of droplets occurring simultaneously so that the average drop size and drop-size distribution probably did not vary too greatly throughout the system. Turbulence in the circulating stream would tend to cause breakup of the particles. The tendency of the dispersed droplets to rise in the continuous phase however is a factor which influences the flow behavior of the dispersion. It might be expected that this factor could be more important in horizontal flow than in vertical flow, since in the former the rising droplets will produce a concentration gradient across the flowing stream. In vertical flow some variation in drop-size distribution might be expected across the stream, particularly in the neighborhood where the low turbulent intensity probably is insufficient to break up the droplets as fast as they coalesce.

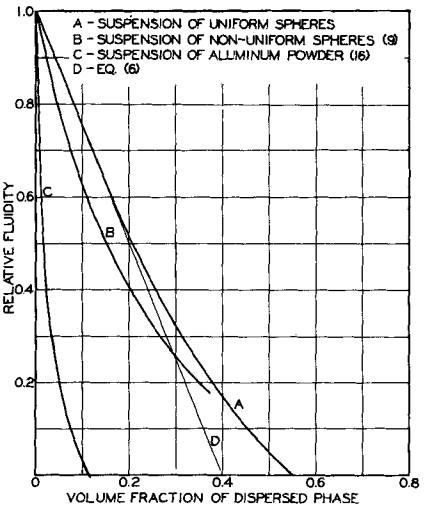

Fig. 1. Fluidity of suspensions of solids.

The various dispersions were studied under laminar and turbulent flow conditions. Friction factors were measured at various flow rates and friction factors were calculated.

In analyzing the data the dispersion is treated as a single-phase fluid, and the usual single-phase friction factor equation was assumed applicable. In treating the dispersion as a single phase fluid, the following assumptions were made:

1 . The dispersed phase is uniformly dispersed throughout the continuous phase.

2. There is no slip between the dispersed and continuous phase so that concentration throughout the system is constant. Samples taken before and after the test section were found to have the same concentration.

3. The droplets are smaller than the scale of turbulence existing in turbulent flow. Baron, et al. (1) have shown for a similar system that droplets of the order of 10 to 25 μ are sufficiently small for the fluid to be considered a single phase. No direct measurements of droplet size were made in the present work. The dispersions had a milk-white appearance and, on the basis of reports of previous investigators, the drop size was probably between 1 and 50 μ. Indirect calculations indicate the size to be of the order of 10 to 25 μ.

The apparent viscosity of the dispersions in laminar flow is calculated from the relationship derived by Langhaar (10):

$$(\mu_m)_{obs} = \frac{\pi r^4 \Delta P\, g_c}{8\, LQ} - 0.149 \cdot \frac{\rho Q}{\pi L} \quad (7)$$

This equation corrects for entrance and exit losses which become significant for short capillary tubes and/or high flow rates.

The apparent viscosity in laminar flow is calculated directly by means of Equation (7) from observed values of ΔP, Q, and the capillary dimensions. In all calculations the density of the dispersion is calculated from the mass fraction of the two liquids present.

Experimental viscosities of water, pure solvent, and various dispersions are plotted in Figure 3 as a function of Reynolds number in the capillary tube. In the two lower charts the lines

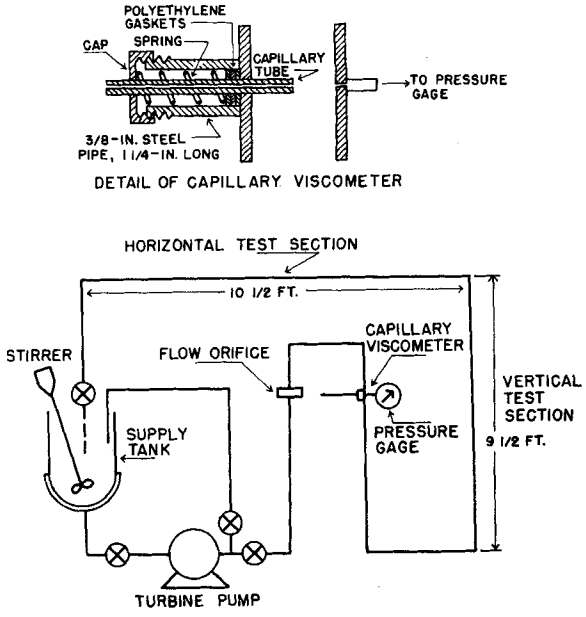

Fig. 2. Flow sheet of test equipment.

correspond to the viscosity of water reported in the literature (*12*) and for viscosity of the pure solvent as measured independently by an Ostwald viscometer. Experimental data agree well with the lines, indicating that the apparatus is operating satisfactorily.

For the 5% emulsion, viscosity is independent of flow rate and tube dimensions. The dispersions containing 20% or more solvent all show a decrease in apparent viscosity with increase in flow rate. In addition there is a dependence of viscosity on tube dimensions and, in the case of the 50% dispersions, a dependence upon tube orientation.

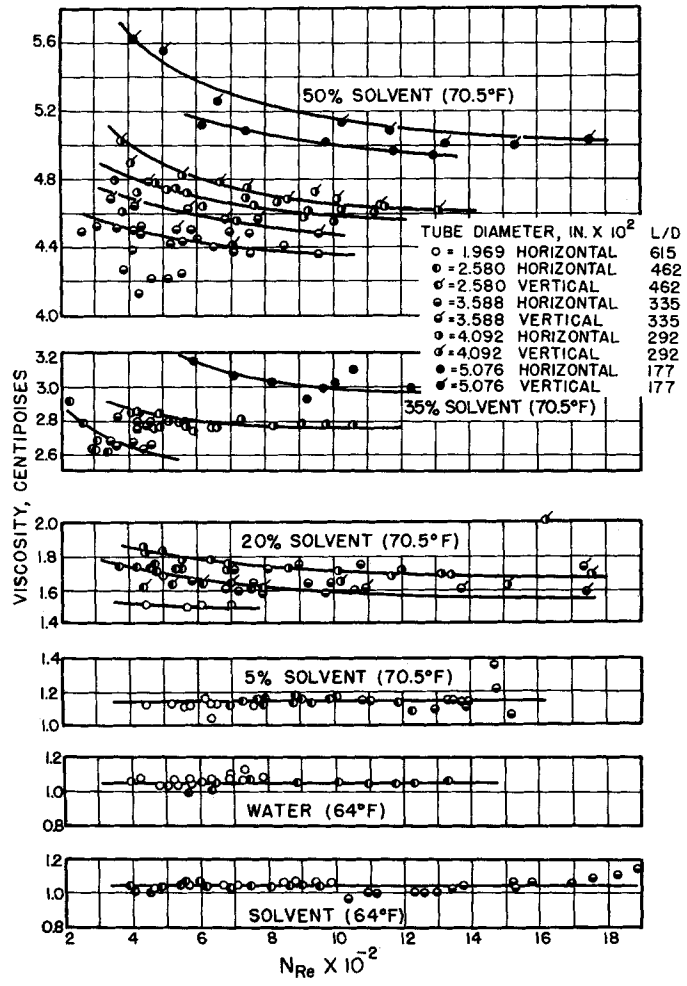

Fig. 3. Laminar flow viscosities of solvent, water, and various dispersions.

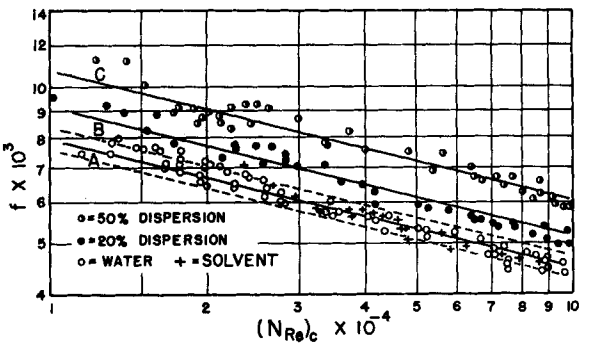

Fig. 4. Turbulent flow friction factors for vertical test section.

Greatest variation of apparent viscosity with flow rate occurs at low Reynolds numbers. In the Reynolds number range between 600 and 1,000 viscosity becomes essentially constant. It is not possible with the present data to determine if the fluid at low flow rates is truly non-Newtonian, or if the decrease of viscosity with flow rate is caused by phase separation and drop coalescence in the capillary. Such effects would become less significant at high flow rates. Further detailed study of the laminar flow regime is necessary.

The variation of observed viscosity with tube orientation can be explained by phase separation or drop coalescence in the capillary tube. The actual behavior in the tube is not known, since no photographic data were obtained on the dispersion entering or leaving the capillary.

For a given tube orientation the observed viscosity increased with tube diameter for concentrations greater than 20% solvent. This is a phenomenon similar to that observed by other investigators (*6, 11, 21*) on suspensions of solids. This is explained on the basis that there is radial migration of the particles toward the tube axis. Such migration has been observed experimentally (*11*) by differences in concentration between inlet and exit of the capillary. Vand (*21*) proposed the following correction for this migration:

$$\frac{\mu_c}{\mu_m} = 1 + \left(1 - \frac{t}{r}\right)^{-4} \left(\frac{\mu_c}{(\mu_m)_{obs}} - 1\right) \qquad (8)$$

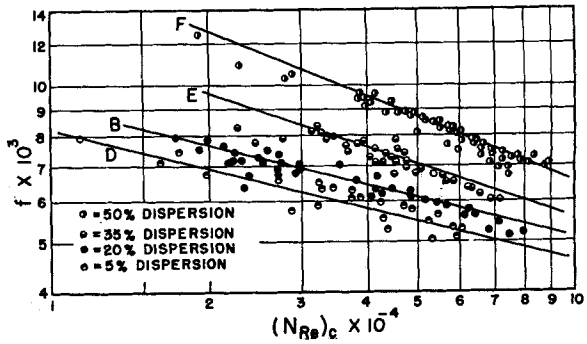

Fig. 5. Turbulent flow friction factors for horizontal test section.

Vand indicated that the thickness of this layer was of the order of the particle diameter. The quantity $(\mu_m)_{obs}$ is the viscosity calculated from Equation (7).

From the data plotted in Figure 3 the value of t is calculated for the 20, 35, and 50% dispersions. These calculations were carried out at Reynolds numbers where $(\mu_m)_{obs}$ had become essentially independent of flow rate. Average values of t were 0.001, 0.0012, and 0.0005 in. for the 20, 35 and 50% dispersions respectively. On the basis of Vand's results the data above indicate a droplet size of the order of 10 to 25 μ. A single value of t however will not bring all the curves in Figure 3 together. If t is taken as 0.0005 in., the curves for the 50% dispersion coincide, but those for the 20 and 35% cases still show about the same spread. The relative fluidities of the various dispersions in laminar flow (at $N_{Re} = 1{,}000$) are plotted in Figure 6. These fluidities are calculated from Equation (8), with $t = 0.0005$ in. These results will be discussed further in conjunction with the turbulent flow results.

The friction factors for turbulent flow are shown in Figures 4 and 5 as a function of the Reynolds number $(N_{Re})_c$ based on the viscosity of the continuous phase. Curve A in Figure 4 represents the relation

$$f = 0.079\ (N_{Re})_c^{-0.25} \qquad (9)$$

which is applicable for single-phase fluids. The water and solvent data agree with this curve within ± 5%, which is the limit represented by the broken lines. It is estimated that the experimental error in the friction factor is ±5%, and therefore the friction factor data for the continuous phases satisfactorily agree with Equation (9). The data for the 20 and 50% dispersions in vertical flow appear to fall parallel to Curve A, and thus Curves B and C in Figure 4 were obtained from a least-square analysis of the data, with a slope of −0.25. The equations of the lines are

For 20% dispersion

$$f = 0.091\ (N_{Re})_c^{-0.25} \qquad (10)$$

For 50% dispersion

$$f = 0.107\ (N_{Re})_c^{-0.25} \qquad (11)$$

It is seen that the data for both of these dispersions follow the respective curves quite well. These dispersions can be treated as Newtonian liquids for vertical turbulent flow. The dispersion flows quickly enough that it is completely mixed. Further since the flow is vertical, droplet rise due to buoyancy has little or no influence.

In Figure 5 the friction factor data for horizontal turbulent flow are presented. Curve B is Equation (10). The data for the horizontal flow of the 20% dispersion follow this curve quite well.

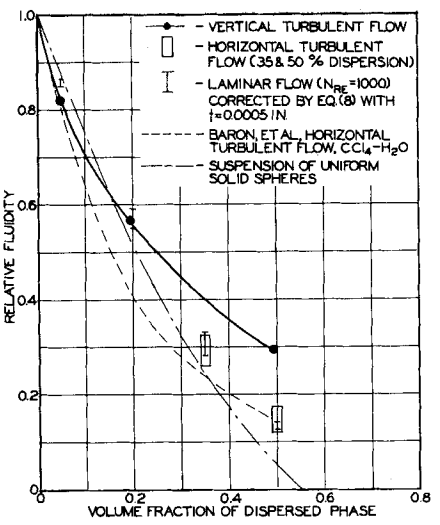

Fig. 6. Relative fluidity of dispersions studied.

Curve D was obtained from a least-square analysis of the data for the 5% dispersion, with a slope of − 0.25:

$$f = 0.082\ (N_{Re})^{-0.25} \qquad (12)$$

These results show that the 5 and 20% dispersions may be treated as Newtonian fluids for horizontal flow as well as for vertical flow.

From Figure 5 it is apparent that the slope of the 35 and 50% data is less than − 0.25. A least-squares analysis yielded the following equations:

For 35% dispersion

$$f = 0.275\ (N_{Re})_c^{-0.338} \qquad (13)$$

For 50% dispersion

$$f = 0.492\ (N_{Re})_c^{-0.368} \qquad (14)$$

In order to calculate the effective viscosity of the dispersions in turbulent flow the general equation of the following form is considered:

$$f = A(N_{Re})_c^{-B} \qquad (15)$$

The apparent viscosity is given such a value that the friction factor Reynolds number relation is the same form as Equation (9); that is

$$f = 0.079(N_{Re})_m^{-0.25} = 0.079(N_{Re})_c^{-0.25}\left(\frac{\mu_c}{\mu_m}\right)^{-0.25} \qquad (16)$$

Combining Equations (15)and (16) one gets

$$\left(\frac{\mu_c}{\mu_m}\right)^{0.25} = \frac{0.079}{A}(N_{Re})_c^{B-0.25} \qquad (17)$$

If $B = 0.25$, the relative viscosity is independent of Reynolds number. However if $B \neq 0.25$, the dispersion displays non-Newtonian characteristics.

The relative fluidities of the various dispersions are plotted in Figure 6. The closed circles represent results obtained from Equations (10), (11), and (12). The solid curve through these points gives the fluidity-concentration relationship of dispersions in vertical flow containing up to 50% solvent, and of dispersions in horizontal flow with up to 20% solvent. The two rectangles at 35 and 50% give the range of fluidities determined from Equations (13) and (14) over the horizontal flow range studied. Laminar flow viscosities corrected by Equation (8), with $t = 0.0005$ in., also are plotted in Figure 6. For comparison the curve for suspensions of uniform spheres and the curve obtained by Baron et al. (*1*) for horizontal turbulent flow of carbon tetrachloride-water dispersions are included.

The fluidities of dispersions in vertical flow (and those up to 20% in horizontal flow) deviate considerably from the curve for uniform spheres. At low concentrations the curve has a slope less than − 2.5. This could be caused by nonuniform size distribution of the droplets as with curve B of Figure 1 for nonuniform solid spheres. At high concentrations the curve for the dispersions is much above the one for suspensions of uniform spheres. It is in this region that viscosity of the dispersed phase apparently has a signifi-

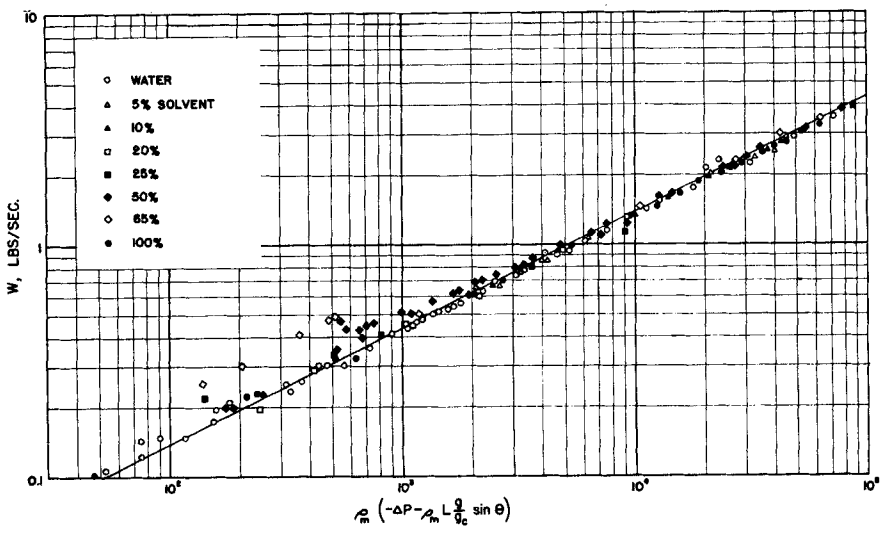

Fig. 7. Orifice calibration.

cant effect. In the case of the dispersions studied in the present work phase inversion occurs in the neighborhood of 60 to 65% solvent, and one might expect a termination of the curve or a discontinuity where the inversion occurs.

The 35 and 50% dispersions in horizontal flow exhibit apparent non-Newtonian behavior. Since this was not observed in vertical flow, the behavior is probably due to phase separation in horizontal flow. Conceivably, stratification could take place with a layer of solvent at the top, a layer of water at the bottom, and an intermediate layer of dispersion with a composition considerably different from the overall composition. The fluidities of the 35 and 50% dispersions in horizontal flow agree reasonably well with the results of Baron et al., who studied horizontal flow of carbon tetrachloride-water dispersions.

The corrected laminar flow fluidities agree well with the turbulent flow results up to 20% concentration. However the 35 and 50% dispersions tend to agree more closely with horizontal turbulent flow data. Explanation of the laminar flow behavior is not possible until a more thorough study of the laminar region is made, particularly with respect to wall effects and coalescence. All dispersions containing greater than 20% solvent displayed non-Newtonian characteristics in laminar flow, which may be real but may also be caused by phase separation, coalescence and radial motion of droplets.

ACKNOWLEDGEMENT

Appreciation is expressed to the National Science Foundation for a grant to carry on this investigation.

NOTATION

A_o = area of orifice, sq.ft.
a = constant in Equation (3)
b = constant in Equation (3)
C = orifice coefficient, dimensionless
D = pipe diameter
D_o = orifice diameter, ft.
du/dy = velocity gradient, sec.$^{-1}$
f = fanning friction factor
g = acceleration of gravity, ft./sec.^{2}
g_c = gravitational conversion factor, lb.$_m$ ft./lb.$_f$sec.^{2}
ΔH = manometer reading, ft.
k = constant in Equation (3)
L = length of capillary tube or test section, distance between pressure taps, ft.
ΔP = total pressure drop across capillary, pressure drop across test section, lb.$_f$/sq. ft.
Q = volumetric flow rate, cu.ft./sec.
$(N_{Re})_m$ = Reynolds number based on viscosity of dispersion
$(N_{Re})_c$ = Reynolds number based on viscosity of continuous phase
r = tube radius, ft.
t = thickness of layer of continuous phase adjacent to tube wall
U = average velocity in tube, ft./sec.
w = mass flow rate, lb.$_m$/sec.

Greek Letters

μ = viscosity, centipoise or lb.$_m$/ft.sec.
μ_c = viscosity of continuous phase
μ_m = viscosity of dispersion
$(\mu_m)_{obs}$ = viscosity calculated from Equation (7)
ϕ = volume fraction of dispersed phase
ρ = density, lb.$_m$/cu.ft.
ρ_h = density of heavy fluid in manometer, lb.$_m$/cu.ft.
ρ_m = density of flowing fluid, lb.$_m$/cu.ft.
ρ_w = density of light fluid in manometer (water in this case), lb.$_m$/cu.ft.
θ = angle that flow line makes with horizontal, radians
τ = shear stress, lb.$_f$/sq.ft.

LITERATURE CITED

1. Baron, Thomas, C. S. Sterling, and A. P. Schueler, "Proceedings Third Midwestern Conference on Fluid Mechanics," pp. 103-123, University of Minnesota Institute of Technology, Minneapolis, Minnesota (1953).
2. Broughton, G., and L. Squires, *J. Phys. Chem.*, **42**, 253 (1938).
3. Cengel, J. A., M.S. thesis, Oregon State College, Corvallis, Oregon (1959).
4. Einstein, A., *Ann. Physik*, **19**, 289 (1906).
5. *Ibid.*, **34**, 391 (1911).
6. Evesen, G. F., R. L. Whitmore, and S. G. Ward, *Nature*, **166**, 1074 (1950).
7. Finnigan, J. W., Ph.D. thesis, Oregon State College, Corvallis, Oregon (1958). (Available on microfilm from University Microfilms, Ann Arbor, Michigan.)
8. Ford, T. F., *J. Phys. Chem.*, **64**, 1168 (1960).
9. Happel, John, *J. Appl. Phys.*, **28**, 1288 (1957).
10. Langhaar, H. L., *Trans. Am. Soc. Mech. Engrs.*, **64**, A-55 (1942).
11. Maude, A. D., and R. L. Whitmore, *Brit. J. Appl. Phys.*, **7**, 98 (1956).
12. McAdams, W. H., "Heat Transmission," 3 ed., McGraw-Hill, New York (1954).
13. Metzner, A. B., and J. C. Reed, *A.I.Ch.E. Journal*, **1**, 434 (1955).
14. Metzner, A. B., *Chem. Eng. Progr.*, **50**, 27 (1954).
15. Oldroyd, J. G., *Proc. Roy. Soc. (London)*, **218A**, 122 (1958).
16. Orr, Clyde, Jr., and J. M. Dallavalle, *Chem. Eng. Progr. Symposium Ser. No. 9*, **50**, 29 (1954).
17. Perry, J. H., "Chemical Engineers' Handbook," McGraw-Hill, New York (1950).
18. Roscoe, R., *Brit. J. Appl. Phys.*, **3**, 267 (1952).
19. Taylor, G. I., *Proc. Roy. Soc.*, **138A**, 41 (1932).
20. Tuve, G. L., and R. E. Sprenkle, *Instruments*, **6**, 201 (1933).
21. Vand, V., *J. Phys. Chem.*, **52**, 277 (1948).
22. Wright, C. H., M.S. thesis, Oregon State College, Corvallis, Oregon (1959).

Manuscript received March 2, 1961; revision received November 27, 1961; paper accepted November 30, 1961. Paper presented at A.I.Ch.E. New York meeting.

APPENDIX

Orifice Calibration

A sharp-edged flow orifice was installed in the experimental equipment and calibrated with dispersions of various concentrations. Mass rate of flow (or lineal velocity if desired) of a single-phase fluid is a function of the pressure drop across the orifice, the fluid density, and the dimensions of the system according to the orifice equation (*17*):

$$w = CA_o \left[\frac{2g_c\rho_m \left(-\Delta P - \rho_m L \frac{g}{g_c} \sin\theta \right)}{1 - (D_o/D)^4} \right]^{1/2} \quad (18)$$

Extensive study (*20*) with single-phase fluids indicates that the coefficient C is constant at approximately 0.61 if the orifice Reynolds number is above 30,000. Below this value it is a function of flow rate and diameter ratio D_o/D.

The 0.695-in. diam. sharp-edged orifice was machined from 1/16-in. brass plate and inserted in a 1¼-in. standard pipe. Vena contracta pressure taps, 1/32 in. in diameter, were connected to differential manometers. Flow was vertically downward through the orifice.

The orifice was calibrated for both pure water and pure solvent and for emulsions containing approximately 5, 10, 20, 25, 50, and 65 volume % of solvent. The estimated errors in the experimental data are: weight ± 0.5%, time ± 0.2%, and pressure drop ± 1.0%.

Since the dispersion has a different density than the fluid in the manometer lines, the following relation holds:

$$-\Delta P - \rho_m L \frac{g}{g_c} \sin\theta = \frac{g}{g_c} [\Delta H(\rho_h - \rho_w) + L(\rho_w - \rho_m)\sin\theta] \quad (19)$$

The vertical separation ($L \sin\theta$) of the pressure taps is a factor which must be considered.

All of the orifice calibration data are shown in Figure 7, where the mass flow rate w is plotted vs. the term $\rho_m\left(-\Delta P - \rho_m L \frac{g}{g_c}\sin\theta\right)$. The data for all fluids studied (except 65% emulsion) agree with the line which represents Equation (18) with $C = 0.61$. This relation may be used for measuring the flow rate of any single-phase liquid and for the solvent-water dispersions containing up to 50% volume % solvent.